

THE TRANSVERSE PARTICLE MIGRATION OF HIGHLY FILLED POLYMER FLUID FLOW IN A PIPE

X. Chen, K.W. Tan, Y. C. Lam, J. C. Chai

Abstract — Shear-induced particle migration was investigated by using a continuum diffusive-flux model for the creep flow of nickel powder filled polymers, which are viscous with shear-thinning characteristic. The model, together with flow equations, was employed for solving the non-Newtonian flow patterns and non-uniform particle concentration distribution of mono-modal suspensions in a pressure-driven tube flow. Particle volume fraction and velocity fields for the non-homogenous shear flow field were predicted for 40% particle volume fraction. The model captures the trends found in experimental investigations.

Keywords: particle migration, diffusion, highly filled polymer

I. INTRODUCTION

Highly filled polymeric systems consisting of solid particulates dispersed in a polymeric matrix are frequently employed in the plastics or metallurgical industry. The flow and deformation of filled polymers have been of interest for many years. The incorporation of solid particulates may critically alter the flow characteristics of the system. Microstructural changes take place during the flow and deformation of even dilute suspensions [1-3]. A systematic investigation of flow of filled compound as a function of rheological properties, deformation rate, volume fraction of particulates, and matrix properties, is of practical importance for the analysis and control of many processing operations [4].

Shear-induced particle migration in the transverse direction, even in the absence of inertial effects, has been well proposed by Leighton and Acrivos [5-6]. Such migration of particles can change the particle concentration distribution, and thus the flow properties of injected articles in the transverse direction. Using Stokesian Dynamics, Nott and Brady [7] have recently performed dynamic simulations of pressure-driven flow for a suspension in a two-dimensional channel with respect to a monolayer of identical spherical non-Brownian particles based on suspension particle temperature balance model. Their simulations confirmed the Leighton and Acrivos shear induced migration theory. Recent work of Hampton et al. [8] reported measurements of initial and fully developed particle concentration and suspension velocity profiles in a circular tube using Nuclear Magnetic Resonance(NMR) imaging techniques.

The results showed particle accumulation and blunting of the velocity profile at the tube center. Other studies of suspensions flowing in rectangular ducts were made using Laser Doppler Anemometry(LDA) techniques [9-10]. In addition, Abbot et al. [11], Phillips et al, [12] and Chow et al. [13] measured concentration profiles of concentrated suspensions in a wide gap Couette device by using NMR. All of them have provided a substantial experimental evidence to support the claim that unimodal suspension of rigid spherical particles generates a nonuniform concentration distribution in non-homogeneous shear flows [14-16].

In this investigation, we extended the particle diffusive model proposed by Phillips et al. [2] by incorporating non-Newtonian viscosity model for a pressure-driven circular channel flow. The investigation indicated that powder concentration variation could be significant and numerical simulation taking into account the change of rheological characteristic of powder/binder mixtures due to particle migration would provide better insight to the flows of non-Newtonian filled polymeric suspension system.

II. GOVERNING EQUATIONS

A. Diffusive flux model

The shear-induced migration of particles is driven by concentration gradients and by shear rate gradients [5-6]. A phenomenological model based on these principles [12] in poiseuille flow yields the particle flux

$$J = -a^2 K_c \mathbf{f} \nabla \left(\mathbf{f} \frac{\partial u}{\partial r} \right) - K_h \mathbf{f}^2 a^2 \frac{\partial u}{\partial r} \frac{\nabla \mathbf{h}}{\mathbf{h}} \quad (1)$$

where u is the velocity of suspension flow, \mathbf{h} the viscosity of suspension, a the particle radius. K_c and K_h are dimensionless phenomenological constants. The dynamic change of particle concentration, \mathbf{f} , along the flow is governed by particle conservation:

$$\frac{D\mathbf{f}}{Dt} = \nabla \cdot \mathbf{J} \quad (2)$$

Following Phillips et al. [8], the implementation of the diffusion equation in pressure driven pipe flow can be written as:

$$\frac{\partial \mathbf{f}}{\partial t} + \frac{\partial(u\mathbf{f})}{\partial z} = \frac{a^2}{r} \left\{ \frac{\partial}{\partial r} [rK_c \dot{\mathbf{g}} \left(\frac{\partial \mathbf{f}}{\partial r} + \frac{\mathbf{f}}{\dot{\mathbf{g}}} \frac{\partial \dot{\mathbf{g}}}{\partial r} \right)] + \frac{\partial}{\partial r} \left(\frac{rK_h \dot{\mathbf{g}}^2 m}{\mathbf{f}_c - \mathbf{f}} \frac{\partial \mathbf{f}}{\partial r} \right) \right\} \quad (3)$$

where a is the particle radius. Shear-induced diffusion is assumed to be independent of interparticle interactions, which include frictional and colloidal forces. These effects are incorporated in the phenomenological constants K_c and K_h of the above equation.

Governing equation (3) must be supplemented with appropriate boundary conditions at the wall, which is subjected to the usual no slip condition, $\mathbf{u} = 0$, and no particle flux through the wall as expressed below:

$$\left\{ \dot{\mathbf{g}} \mathbf{f} \left(K_c + \frac{K_h \mathbf{f} m}{\mathbf{f}_c - \mathbf{f}} \right) \frac{\partial \mathbf{f}}{\partial r} + K_c \mathbf{f}^2 \frac{\partial \dot{\mathbf{g}}}{\partial r} \right\} \cdot \mathbf{n} = 0 \quad (4)$$

where \mathbf{n} is the outward normal unit vector.

Particle concentration \mathbf{f} is assumed to be uniform initially at the entrance of the tube, i.e.

$$\mathbf{f} = \mathbf{f}_0, \text{ for } 0 \leq r \leq R, \text{ at } z = 0. \quad (5)$$

B. Flow equations

The flow of concentrated suspension fluids in viscometric equipment takes place at low particle Reynolds numbers ($Re \ll 1$), and the creeping flow approximation is applicable [17]. Thus the conservation equations for steady, incompressible flow rate are [12]:

$$\nabla \cdot \bar{\mathbf{u}} = 0, \quad (6)$$

$$-\nabla p + \nabla \cdot \bar{\bar{\mathbf{T}}} = 0 \quad (7)$$

where $\bar{\mathbf{u}}$ is the velocity vector, p is the hydrostatic pressure, $\bar{\bar{\mathbf{T}}}$ is the extra stress tensor. Considering a non-Newtonian fluid, the extra stress tensor $\bar{\bar{\mathbf{T}}}$ is given by:

$$\bar{\bar{\mathbf{T}}} = \mathbf{h}(\dot{\mathbf{g}}, T, \mathbf{f}) \bar{\bar{\mathbf{g}}} \quad (8)$$

where \mathbf{h} is the apparent viscosity, which is a function of temperature T , particle concentration \mathbf{f} and the rate-of-strain tensor $\bar{\bar{\mathbf{g}}} = \nabla \bar{\mathbf{u}} + (\nabla \bar{\mathbf{u}})^T$.

The functional relationship of \mathbf{h} can take several forms that adequately model viscosity data for concentrated suspension fluids (e.g. Krieger model) [18]. A viscosity formulation of a concentrated suspension that is described by the Krieger model [18] is adopted here:

$$\mathbf{h} = \mathbf{h}_b \left(1 - \frac{\mathbf{f}}{\mathbf{f}_c} \right)^{-m} \quad (9)$$

where \mathbf{h}_b is the viscosity of the binder system, \mathbf{f} is particle concentration, \mathbf{f}_c is the critical loading of the particle. m is a material constant. For this investigation, \mathbf{f}_c was assumed to be 0.68. For the determination of the material constant m in equation (2), it is important to carry out experiments under the conditions that there is no or minimum particle migration. As it was shown [13] that parallel-plate viscometer introduced little migration, m was determined to be 0.82.

The modified Cross model can be employed to describe the viscosity of the binder, which describes a shear-thinning behavior:

$$\mathbf{h}_b = \frac{\mathbf{h}_0}{1 + (\mathbf{h}_0 \dot{\mathbf{g}} / \mathbf{t}^*)^{1-n}} \quad (10)$$

with

$$\mathbf{h}_0 = B \exp(T_b / T) \quad (11)$$

where B, T_b and \mathbf{t}^* are material constants. The viscosity at zero shear-rate, \mathbf{h}_0 , is used in this model. At high shear rate, the equation (10) can be modified into [20]:

$$\mathbf{h}_b = (\mathbf{h}_0 \dot{\mathbf{g}}_0^{1-n}) \dot{\mathbf{g}}^{n-1} \quad (12)$$

where $\dot{\mathbf{g}}_0 = \mathbf{t}^* / \mathbf{h}_0$. Equation (12) is a power law model which also can describe the rheological behaviour of suspension at high shear rate.

III. EXPERIMENTAL TECHNIQUES

To measure transverse shear-induced particle migration, the particle distribution was quantified by conducting experiments using viscous nickel (Ni-171) spherical particles having a sieved mean size of 58 μm suspended in a non-Newtonian solvent composed of Ethylene Vinyl Acetate (EVA460) resin manufactured by Dupont. The particle concentration of 0.4 volume fraction was used in this investigation. The viscous suspensions were initially mixed using the Haake Rheomix600 torque mixer. The chamber temperature was set at 180°C and a rotary speed of 50 rpm to ensure thorough mixing.

To determine the material constants of the rheological model, experiments were conducted using parallel plate rheometer for the non-Newtonian solvent. Various concentrations were used. With these rheometric experimental data, the material index, m of Equation (9) of the model was determined.

The extrusion process was conducted on a capillary rheometer to characterize flow behaviour of the feedstock with specially designed split dies. The capillary split die with an inner die radius of 1.5mm and length of 40mm

was used to characterize particle migration. Experiments were repeated 3 times after which the averaged results were computed. After injection, the feedstock samples were amassed from the split dies as shown in Figure 1. They were then stored inside a desecrator to maintain in a dry condition. Subsequently, the samples were sliced into 5mm interval for the whole length. To increase the electrical conductivity of the feedstock samples, a sputter coater was utilized. Thereafter, SEM was employed to capture micrographs for the determination of the radial

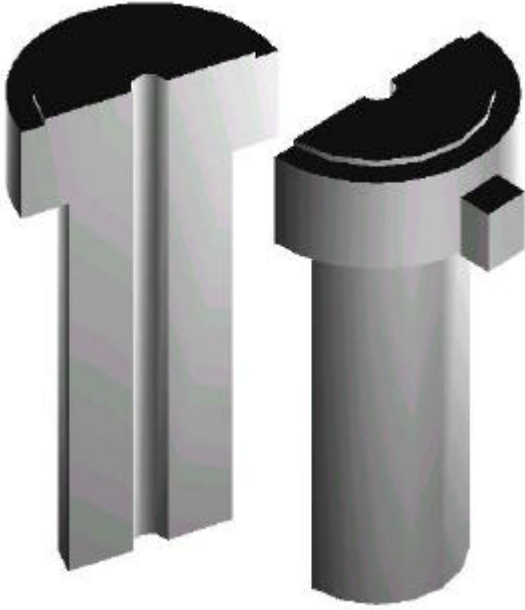


Figure 1: Capillary Half Split Die.

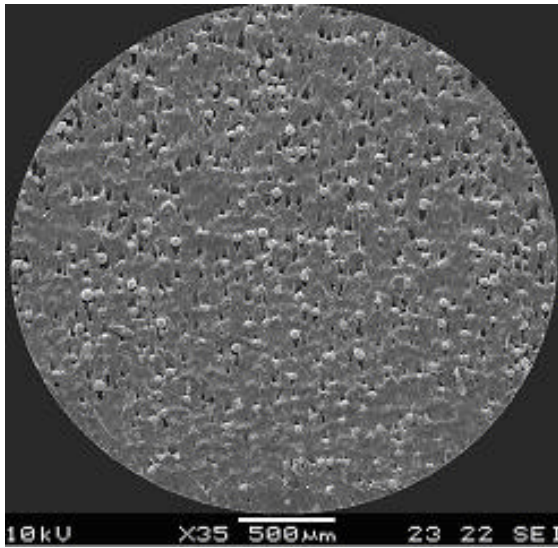


Figure 2 Morphology of Ni-171 Spherical Particles suspended in EVA460 Binder Matrix for $\bar{\Phi} = 40\%$ at the Exit Section of Tube.

particle distribution that was measured using image analyzer software (Image ProPlus). Figure 2 shows the nickel sample morphologies suspended in EVA460 binder at the exit sections for a concentration of 40%.

IV. RESULTS AND DISCUSSION

The rheological constants $B = 2530.7(g \cdot cm^{-1}s^{-1})$, $T_b = 2636.1K$ (in equation (11)), $t^* = 28733.86(g \cdot cm^{-1}s^{-2})$, $n = 0.385$ (in equation (10)) of the EVA 460

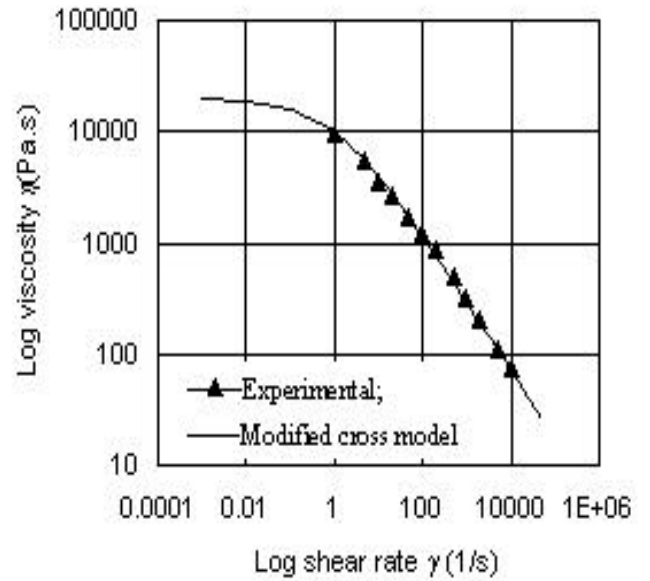


Figure 3 Rheological behaviour of EVA420 binder at $180^\circ C$

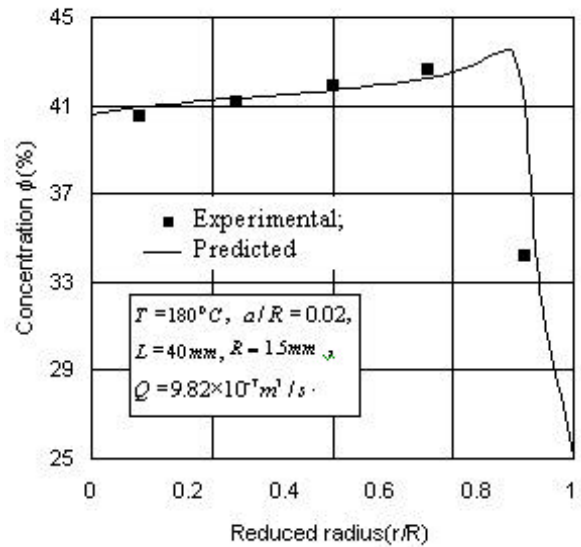


Figure 4 Concentration profile at exit section ($z=1.0$) for $\bar{F} = 40\%$.

binder system were determined by data fitting of viscosity measurement shown in Figure 3 using the modified Cross model. The value of material constant, m was determined to be 0.82 from parallel plate experiments. For EVA460, the fluid exhibits Newtonian plateau value at low shear rate and shear thinning at high shear rate. As shown in Figure 3, the modified cross model can fit the experimental data well at both low and high shear rates.

Figure 4 shows the comparisons of simulation and experimental results for particle concentration 40% in the radial direction at the exit section. It was experimentally observed a decrease in concentration at the wall with a corresponding increase in concentration at the region next to the wall. The experimental observations were obtained at five layers in the radial direction of the sample with the center of layers at reduced radius $r/R = 0.1, 0.3, 0.5, 0.7$ and 0.9 respectively.

The empirical constants K_c and K_h in the diffusion equation (3) were obtained by fitting particle concentration data between experimental observations and numerical predictions [8]. Through this approach, the values $K_c = 0.33$, $K_h = 0.65$ ($K_c/K_h = 0.51$) were obtained.

Both experimental and numerical results showed a near plug-like concentration profile for non-Newtonian concentrated suspension during pressure-driven tube flow. The shape is quite different from a cusp-like profile of concentration predicted at the centerline of the tube where

rate at the wall, which amplified particle migration near the wall. As shown in Figure 4, the numerical model could capture this feature.

In order to ensure that accurate pressure data were obtained and to investigate the predictive capabilities of the model for a different geometry, a standard die of 1 mm in diameter and 30mm in length was employed. Figure 5 shows comparison of pressure drop versus flowrate between predicted and experimental data and the results indicated that numerical prediction over-estimated the pressure where migration was not considered. Taking into consideration of particle migration, the agreement between numerical prediction and experimental observations were good. This is because of higher flow conductance due to particle migration. This is a result of a higher concentration of lower viscosity polymer at the region near the wall of the tube. Therefore, it was evident that the present model was capable of tracking this prominent effect in a concentrated suspension in non-homogenous shear flow.

At any position along the tube, concentration distribution and the velocity profile in the cross section have not yet attained their final steady state profiles. Figure 6 shows the development of velocity profiles at different reduced length $z=0, 1.0$ and velocity profile at a fully developed flow, which length can be scaled as R^3/a^2 [14]. As the particle traveling down the tube, the velocity profiles were blunted. This is because of the

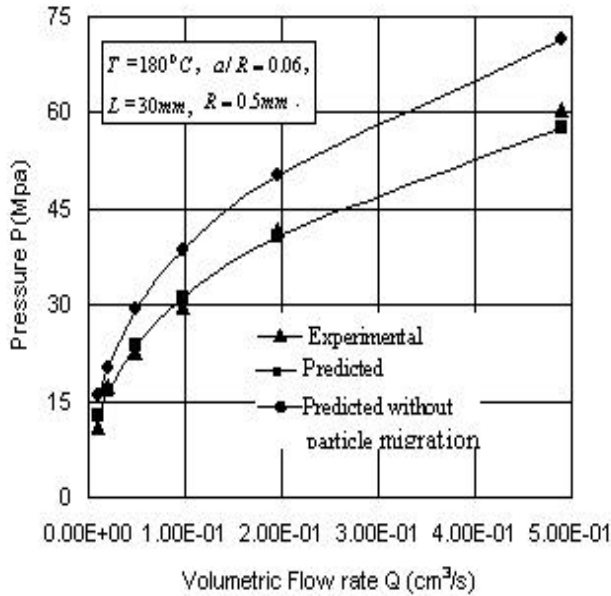


Figure 5 Comparison of pressure drop versus flowrate between predicted and experimental data for $\bar{F} = 40\%$.

the local shear rate vanished for Newtonian suspension fluids ($n=1$)[12]. This is due to the effect of shear-thinning of non-Newtonian fluid. The effect of shear thinning is to decrease the viscosity and increase the shear

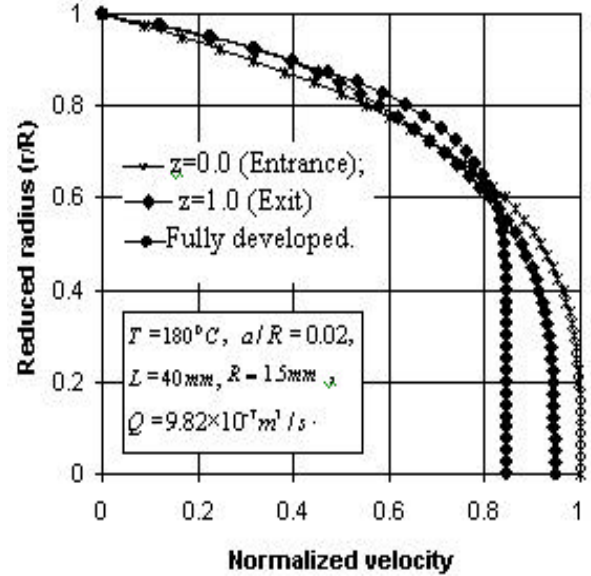


Figure 6 Predicted velocity profiles at different reduced length (z) for $\bar{F} = 40\%$. The velocity is normalized with respect to the maximum velocity at entrance ($z=0.0$).

changes of concentration of particle due to particle migration away from the wall of the tube. The resulting effective viscosity in the cross section of the tube becomes highly non-uniform, which is higher at the center of the tube and lower at the wall. This is reflected in the

flattening of the velocity profile at the center of the tube. At the fully developed state, the flow at the region of high concentration resembles a near plug-like flow of a solid core.

For a fully developed, steady state, pressure-driven fluid tube flow using power-law model, the analytical solution to equation (3) can be obtained as:

$$\frac{r}{R} = \left(\frac{f_w}{f} \right)^n \left(\frac{f_c - f_w}{f_c - f} \right)^{\frac{mn(K_h - 1)}{n}} \quad (13)$$

where R is the radius of the tube and f_w is the concentration at the wall. This analytical solution for power-law fluid is different from that given by the original model [12] for the Newtonian fluid in that the non-Newtonian index n has an effect on concentration profile. Figure 7 shows a comparison of predicted concentration profiles for particle concentration 40% with different non-Newtonian index n . When $n=1$, i.e. Newtonian fluid, the cusp-like concentration profile was predicted as expected as in the model of Phillips et al [12]. With the index n decreases ($n<1$), the cusp-like profile at the center of the tube was flattened gradually. It is observed that the effect of non-Newtonian index n is to relax the cusp-like appearance in the concentration profile at the center of the tube.

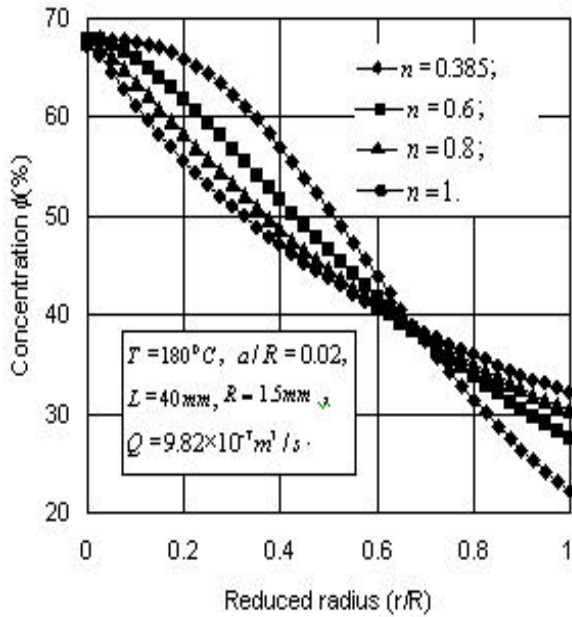


Figure 7 Effect of non-Newtonian index n on steady state profiles of particle concentration in radial direction for $\bar{F} = 40\%$.

Figure 8 shows the deviation \hat{f} of particle concentration versus reduced length ($z=l/L$) at the volumetric flowrate $Q = 9.82 \times 10^{-1} \text{ cm}^3 / \text{s}$ with initial particle concentration

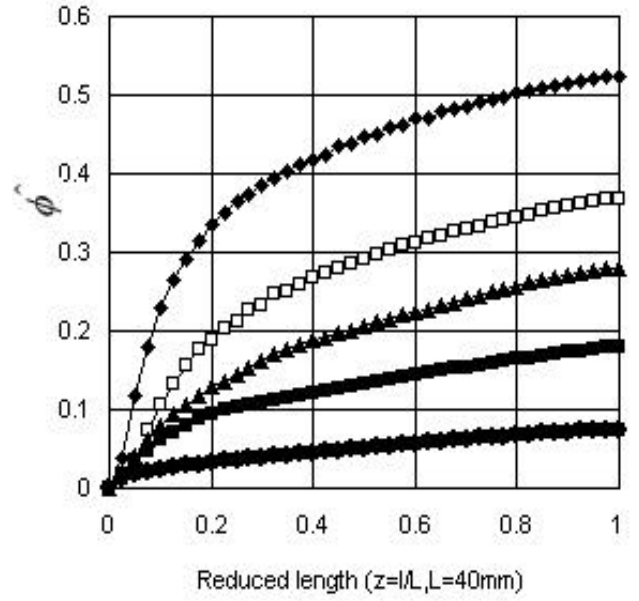


Figure 8(a) Predicted \hat{f} at various a/R ratio for bulk concentration $\bar{F} = 40\%$. Predictions at (a/R) ratio: \blacklozenge -0.08; \square -0.04; \blacktriangle -0.02; \blacksquare -0.01; \bullet -0.005.

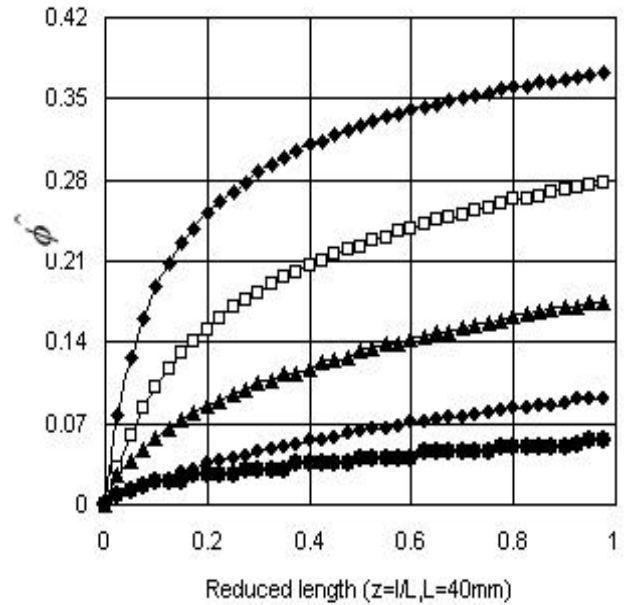


Figure 8(b) Predicted \hat{f} at various a/R ratio for bulk concentration $\bar{F} = 50\%$. Predictions at (a/R) ratio: \blacklozenge -0.08; \square -0.04; \blacktriangle -0.02; \blacksquare -0.01; \bullet -0.005.

40% and 50% for various values of a/R . \hat{f} was defined as $(\bar{f} - \bar{f}_w) / \bar{f}$, that is the deviation of particle concentration \bar{f}_w at the wall from the bulk concentration

\bar{f} . With increasing value of a/R , the deviation \hat{f} increases. The deviation \hat{f} is relatively small (≤ 0.1) if the value of a/R is below 0.005. This means that if a/R is small, there will be little particle migration.

The deviation \hat{f} decreases for increasing initial values of particle concentration at a specified value of a/R . As shown in Figures 8 (b), with a lower initial particle concentration (40%), the deviation of particle concentration is around 0.52 for the value of $a/R = 0.08$ at the exit section of the tube. \hat{f} is more than 0.37 for initial particle concentration of 50%.

V. CONCLUSION

The complex behavior of a suspension containing sphere particles was simulated using diffusive-flux modeling. This model couples a generalized Newtonian stress/strain relationship with shear-induced migration model of the suspended particles in which the local effective viscosity is dependent on the local volume fraction of the particles. The shear-induced particle migration model could capture the essential features in pressure-driven suspension tube flow. The model, with the material constants determined, was demonstrated to have good agreement with experiment results. The results indicated that particle migration could be a significant phenomenon. If it is ignored, significant error could exist in particle concentration distribution and pressure predicted.

REFERENCES

1. Karnis, A., H.L. Goldsmith, and S.G. Mason, The Kinetics of Flowing Dispersions: I Concentrated Suspensions of Rigid Particles, *J. Colloid Interface Sci.*, vol. 22, pp. 531-553, 1966.
2. Hookham, P.A., Concentration and Velocity Measurements in Suspensions Flowing Through a Rectangular Channel, Ph.D thesis, California Institute and Technology, 1986.
3. Gadala-Maria, F. and A. Acrivos, Shear-induced Structure in a Concentrated Suspension of Solid Spheres, *J. Rheol.*, vol. 24, pp. 799-811, 1980.
4. Randall M. German, Metal Powder Industries Federation, *Princeton*, N.J, 1991.
5. Leighton, D. and Acrivos A., The shear-induced self-diffusion in concentrated suspensions. *J. Fluid Mech.*, vol. 181, pp. 415-439, 1987.
6. Leighton, D. and Acrivos A., Measurement of shear-induced self-diffusion in concentrated suspensions of spheres. *J. Fluid Mech.*, vol. 177, pp. 109-131, 1987.
7. Nott P. R. and Brady J.F., Pressure-driven flow of suspensions: simulation and theory, *J. Fluid Mech.*, vol. 275, pp. 157-199, 1994.
8. Hampton R.E., Mammoli A.A., Graham A.L. and Tetlow N., Migration of particles undergoing pressure-driven flow in a circular conduit, *J. Rheol.*, vol. 41, pp. 621-640, 1997.
9. Koh. C, L.G. Leal and P.A. Hookham, An Experimental Investigation of Concentrated Suspension Flow in a Rectangular Channel, *J Fluid Mech.*, vol. 256, pp. 1-32, 1994
10. Averbakh, A., Shauly, A., Nir, A. and Semiat R, Slow viscous flows of highly concentrated suspensions-part II: particle migration, velocity and concentration profiles in rectangular ducts, *Int. J. Multiphase flow*, vol. 23, pp. 613-629, 1997.
11. Abbot, J.R., Tetlow, N., Graham, A. L., Altobelli, S.A., Fukushima, E., Mondy, L. A. & Stephens, T.A., Experimental observations of particle migration in concentrated suspensions: couette flow, *J. Rheol.*, vol. 35, pp. 773-795, 1991.
12. Phillips R.J., Armstrong R. C., Brown R.A., Graham, A.L. and Abbot, J.R., A Constitutive Equations for Concentrated Suspensions that Accounts for Shear-induced Particle Migration, *Phys. Fluids A*, vol. 4, pp. 30-40, 1992.
13. Chow A.W, Sinton S.W, Iwamiya J H, Shear-induced particle migration in Couette and parallel plate viscometers: NMR imaging and stress measurements, *Phys. Fluids, A*, vol. 6, pp. 2561-2575, 1994.
14. N. Phan-Thien, A brief review of suspension mechanics, 7th National Conference on Rheology, Brisbane, pp. 7-10, 1994.
15. Fang Z and N. Phan-Thien, A particle suspension model: an unstructured finite-volume implementation, *J. Non-Newtonian Fluid Mech.*, vol. 80, pp. 135-153, 1999.
16. Allende M. and Kalyon D.M., Assessment of particle-migration effects in pressure-driven viscometric flows, *J. Rheology*, vol. 44, pp. 79-90, 2000.
17. H.P. Wang, and H.S. Lee, Numerical Techniques for Free and Moving Boundary Problems, C.L. Tucker III, editor. Carl Hanser Verlag, Munich, 1989.
18. Krieger, I. M, Adv., Rheology of monodisperse lattice, *Adv. Colloid Interface Sci*, vol 3, pp. 111-136, 1972.
19. Patanker S. V., Numerical heat transfer and fluid flow, Hemisphere Pub. Co., New York, McGraw-Hill, 1980.
20. Christopher W. M., Rheology: Principles, Measurements, and Applications, VCH publisher inc, 1994.

X. Chen: Ph.D, Reserch Fellow, Singapore-MIT Alliance Programme, Nanyang Technological University, Singapore 639798

K.W.Tan: Research Student, School of Mechanical & Production Engineering, Nanyang Technological University, Singapore 639798

Y.C. Lam: Ph.D, Professor, SMA Fellow, Singapore-MIT Alliance Programme, Nanyang Technological University, Singapore 639798

J.C. Chai: Ph.D, Associate Professor, School of Mechanical and Production Engineering, Nanyang Technological University, Singapore 639798